



PD+ attitude control of rigid bodies with improved performance

Rune Schlanbusch, Antonio Loria, P. J. Nicklasson

► To cite this version:

Rune Schlanbusch, Antonio Loria, P. J. Nicklasson. PD+ attitude control of rigid bodies with improved performance. 49th IEEE Conference on Decision Control, Dec 2010, Atlanta, United States. pp.7069-7074. hal-00521521

HAL Id: hal-00521521

<https://hal-centralesupelec.archives-ouvertes.fr/hal-00521521>

Submitted on 28 Mar 2011

HAL is a multi-disciplinary open access archive for the deposit and dissemination of scientific research documents, whether they are published or not. The documents may come from teaching and research institutions in France or abroad, or from public or private research centers.

L'archive ouverte pluridisciplinaire **HAL**, est destinée au dépôt et à la diffusion de documents scientifiques de niveau recherche, publiés ou non, émanant des établissements d'enseignement et de recherche français ou étrangers, des laboratoires publics ou privés.

PD+ Attitude Control of Rigid Bodies with Improved Performance

Rune Schlanbusch, Antonio Loria, Raymond Kristiansen and Per Johan Nicklasson

Abstract—We address the problem of state feedback attitude control of a rigid body in quaternion coordinate space through a modified PD+ tracking controller. The control law ensures faster convergence to the desired operating point during attitude maneuver, while keeping the gains small for station keeping. A direct consequence is a drop in energy consumption when affected by sensor noise. More precisely, we show uniform asymptotic stability for the system without perturbations and uniform practical asymptotic stability in the presence of unknown, bounded input disturbances. Simulation results illustrate the performance improvement with respect to classic PD+ control, especially in the presence of input perturbations.

I. INTRODUCTION

Attitude control on the rotational sphere is an interesting theoretical problem since, due to the parametrization of the attitude for the unit quaternion, the model has multiple equilibrium points. From a more practical viewpoint, besides achieving stability in some sense, control of a rigid body demands fast and accurate settling using minimal effort. Thus, a wide number of controllers have been developed during the past years, by focusing on the enhancement of performance while guaranteeing robust stability and minimizing the control effort.

Attitude tracking control naturally lies on a bulk of literature on tracking control of robot manipulators and, more generally Euler-Lagrange systems –cf. [1]. A classic in robot control literature is the PD+ controller of Paden and Panja –cf. [2] which, together with the Slotine and Li controller –[3], was the first algorithm for which global asymptotic stability was demonstrated. A PD+ based controller for spacecraft was presented in [4], called model-dependent control, and more recently for leader-follower spacecraft formation in [5].

In this paper we use a modified PD+ controller which, roughly speaking, includes nonlinear gains of exponential growth. That is, for large errors the controller ensures fast convergence; on the other hand, the control effort is reduced exponentially in a neighborhood of the reference operating point. Consequently, very little control effort is used in station-keeping tasks, especially in the presence of sensor noise. Strictly speaking, we show that the origin of the closed-loop system is uniformly practically asymptotically stable with respect to perturbations. Our theoretical findings are validated in simulation for an Earth orbiting spacecraft.

Rune Schlanbusch, Raymond Kristiansen and Per Johan Nicklasson are with Department of Technology, Narvik University College, PB 385, AN-8505 Narvik, Norway {runsch, rayk, pjn}@hin.no

Antonio Loria is with CNRS, LSS-Supélec, 3, Rue Joliot Curie, 91192 Gif s/Yvette, France loria@lss.supelec.fr

A range of results are presented to compare performance of the modified PD+ controller relative to the classical one.

II. PRELIMINARIES

The cross product operator \times between two vectors \mathbf{a} and \mathbf{b} is written as $\mathbf{S}(\mathbf{a})\mathbf{b}$ where \mathbf{S} is skew-symmetric. The symbol $\omega_{b,a}^c$ denotes angular velocity of frame a relative to frame b , expressed in the frame c ; \mathbf{R}_a^b is the rotation matrix from frame a to frame b ; $\|\cdot\|$ denotes the Euclidean norm. Coordinate reference frames are denoted by $\mathcal{F}^{(\cdot)}$, where the superscript denotes the frame in question. When the context is sufficiently explicit, we omit the arguments of functions.

A. Cartesian Coordinate Frames

The coordinate reference frames used throughout the paper are defined as follows:

Earth-centered inertial frame: The Earth-centered inertial (ECI) frame is denoted \mathcal{F}^i , and has its origin in the center of the Earth. The axes are denoted \mathbf{x}^i , \mathbf{y}^i , and \mathbf{z}^i , where the \mathbf{z}^i axis is directed along the axis of rotation of the Earth toward the celestial North Pole, the \mathbf{x}^i axis is pointing in the direction of Υ , which is the vector pointing from the center of the Sun toward the center of the Earth during the vernal equinox, and finally the \mathbf{y}^i axis complete the right handed orthonormal frame.

Spacecraft orbit reference frame: The orbit frame, denoted \mathcal{F}^o , has its origin located in the center of mass of the spacecraft. The \mathbf{x}^o axis in the frame coincide with the vector $\mathbf{r}^i = [r_x, r_y, r_z]^\top \in \mathbb{R}^3$ from the center of the Earth to the spacecraft, and the \mathbf{z}^o axis is parallel to the orbital angular momentum vector, pointing in the orbit normal direction. The \mathbf{y}^o axis completes the right-handed orthonormal frame. The basis vectors of the frame can be defined as

$$\mathbf{x}^o := \frac{\mathbf{r}^i}{r}, \quad \mathbf{y}^o := \mathbf{S}(\mathbf{z}^o)\mathbf{x}^o \quad \text{and} \quad \mathbf{z}^o := \frac{\mathbf{h}^i}{h}, \quad (1)$$

where $\mathbf{h}^i = \mathbf{S}(\mathbf{r}^i)\dot{\mathbf{r}}^i \in \mathbb{R}^3$ is the angular momentum vector of the orbit, $h = \|\mathbf{h}^i\|$ and $r = \|\mathbf{r}^i\|$. This frame is also known as the Local Vertical/Local Horizontal (LVLH) frame.

Body reference frame: The body frame is denoted \mathcal{F}^b , and is located at the center of mass of the rigid body, and its basis vectors are aligned with the principle axis of inertia.

Auxiliary orbit frame: Because of the nature of the aerodynamic drag and the fact that it always acts along the velocity vector of the spacecraft we need an auxiliary orbit frame, denoted \mathcal{F}^a , when elliptic orbits are considered. The first basis vector is parallel with the orbit frame such that $\mathbf{x}^a \parallel \mathbf{x}^o$,

\mathbf{y}^a is pointing in the direction of the spacecraft velocity vector, and \mathbf{z}^a is completing the right-handed orthonormal frame. A rotation between the auxiliary frame and the LVLH frame is expressed as [6]

$$\mathbf{C}_a^o = \frac{h}{pv} \begin{bmatrix} \frac{p}{r} & e \sin \nu & 0 \\ -e \sin \nu & \frac{p}{r} & 0 \\ 0 & 0 & \frac{pv}{h} \end{bmatrix}, \quad (2)$$

where $p = h^2/\mu$ is the semi-latus rectum of the spacecraft orbit, μ is the geocentric gravitational constant of the Earth, v is the magnitude of the velocity vector, e is the orbit eccentricity, and ν is the true anomaly. Note that \mathbf{C}_a^o is not in general a proper rotation matrix since

$$\det \mathbf{C}_a^o = 1 + e^2 + 2e \cos \nu.$$

B. Quaternions

The attitude of a rigid body is often represented by a rotation matrix $\mathbf{R} \in SO(3)$ fulfilling

$$SO(3) = \{\mathbf{R} \in \mathbb{R}^{3 \times 3} : \mathbf{R}^\top \mathbf{R} = \mathbf{I}, \det \mathbf{R} = 1\},$$

which is the special orthogonal group of order three. Quaternions are often used to parameterize members of $SO(3)$ where the unit quaternion is defined as $\mathbf{q} = [\eta, \boldsymbol{\epsilon}^\top]^\top \in S^3 = \{\mathbf{x} \in \mathbb{R}^4 : \mathbf{x}^\top \mathbf{x} = 1\}$, where $\eta \in \mathbb{R}$ is the scalar part and $\boldsymbol{\epsilon} \in \mathbb{R}^3$ is the vector part. The rotation matrix may be described by [7]

$$\mathbf{R} = \mathbf{I} + 2\eta \mathbf{S}(\boldsymbol{\epsilon}) + 2\mathbf{S}^2(\boldsymbol{\epsilon}) \quad (3)$$

with $\boldsymbol{\epsilon} = [\epsilon_x, \epsilon_y, \epsilon_z]^\top$, where the matrix $\mathbf{S}(\cdot)$ is the cross product operator

$$\mathbf{S}(\boldsymbol{\epsilon}) = \boldsymbol{\epsilon} \times = \begin{bmatrix} 0 & -\epsilon_z & \epsilon_y \\ \epsilon_z & 0 & -\epsilon_x \\ -\epsilon_y & \epsilon_x & 0 \end{bmatrix}.$$

The inverse rotation can be performed by using the inverse conjugated of \mathbf{q} as $\bar{\mathbf{q}} = [\eta, -\boldsymbol{\epsilon}^\top]^\top$. The set S^3 forms a group with quaternion multiplication, which is distributive and associative, but not commutative, and the quaternion product of two arbitrary quaternions \mathbf{q}_1 and \mathbf{q}_2 is defined as [7]

$$\mathbf{q}_1 \otimes \mathbf{q}_2 = \begin{bmatrix} \eta_1 \eta_2 - \boldsymbol{\epsilon}_1^\top \boldsymbol{\epsilon}_2 \\ \eta_1 \boldsymbol{\epsilon}_2 + \eta_2 \boldsymbol{\epsilon}_1 + \mathbf{S}(\boldsymbol{\epsilon}_1) \boldsymbol{\epsilon}_2 \end{bmatrix}.$$

It must be noted that the quaternion representation is inherently redundant therefore, it admits two mathematically different equilibria $\mathbf{q}_1 \otimes \mathbf{q}_2 = [\pm 1, \mathbf{0}]^\top$ which in fact represent the exact same physical orientation *i.e.*, one is rotated by 2π rad relative to the other about an arbitrary axis.

C. Kinematics and Dynamics

The time derivative of (3) can be written as [7]

$$\dot{\mathbf{R}}_b^a = \mathbf{S}(\boldsymbol{\omega}_{a,b}^a) \mathbf{R}_b^a = \mathbf{R}_b^a \mathbf{S}(\boldsymbol{\omega}_{a,b}^b),$$

and the kinematic differential equations can be expressed as [7]

$$\dot{\mathbf{q}} = \mathbf{T}(\mathbf{q}) \boldsymbol{\omega}_{i,b}^b, \quad (4)$$

where

$$\mathbf{T}(\mathbf{q}) = \frac{1}{2} \begin{bmatrix} -\boldsymbol{\epsilon}^\top \\ \eta \mathbf{I} + \mathbf{S}(\boldsymbol{\epsilon}) \end{bmatrix} \in \mathbb{R}^{4 \times 3}.$$

The dynamical model of a rigid body can be described by a differential equation for angular velocity, and is deduced from Euler's moment equation. This equation describes the relationship between applied torque and angular momentum on a rigid body as [8]

$$\mathbf{J} \dot{\boldsymbol{\omega}}_{i,b}^b = -\mathbf{S}(\boldsymbol{\omega}_{i,b}^b) \mathbf{J} \boldsymbol{\omega}_{i,b}^b + \boldsymbol{\tau}^b \quad (5)$$

$$\boldsymbol{\omega}_{o,b}^b = \boldsymbol{\omega}_{i,b}^b - \mathbf{R}_i^b \boldsymbol{\omega}_{i,o}^i, \quad (6)$$

$$\boldsymbol{\omega}_{i,o}^i = \frac{\mathbf{S}(\mathbf{r}^i) \mathbf{v}^i}{\mathbf{r}^{i,\top} \mathbf{r}^i},$$

where $\mathbf{v}^i \in \mathbb{R}^3$ is the spacecraft velocity vector in inertial frame, $\boldsymbol{\tau}^b \in \mathbb{R}^3$ is the total torque working on the body frame, and $\mathbf{J} = \text{diag}\{j_x, j_y, j_z\} \in \mathbb{R}^{3 \times 3}$ is the inertia matrix where j_x, j_y and j_z are the moments of inertia of the body about its three orthonormal axes. The torque working on the body is expressed as $\boldsymbol{\tau}^b = \boldsymbol{\tau}_a^b + \boldsymbol{\tau}_d^b$, where $\boldsymbol{\tau}_d^b$ is the disturbance torque, and $\boldsymbol{\tau}_a^b$ is the actuator (control) torque. Usually the desired trajectory is given in the orbit frame such as $\boldsymbol{\omega}_{o,d}^o$, which means that (6) has to be used as state, which leads to an increased complexity of the control structure as in [9]. Instead we add (6) and its derivative to the generated reference such that $\boldsymbol{\omega}_{i,d}^b = \mathbf{R}_i^b \boldsymbol{\omega}_{i,o}^i + \mathbf{R}_o^b \boldsymbol{\omega}_{o,d}^o$. Throughout the paper we will denote $\boldsymbol{\omega} = \boldsymbol{\omega}_{i,b}^b$.

D. Disturbances

Since a spacecraft in an elliptic Low Earth Orbit (LEO) is considered for our simulations, we only consider the disturbance torques which are the major contributors to these kind of orbits, namely: gravity gradient, and torques caused by atmospheric drag and J_2 effect. Gravity gradient torque is forcing the spacecraft to align its axis of minimum moment of inertia vertically and can be expressed as [8]

$$\boldsymbol{\tau}_{gg}^b = \mathbf{R}_i^b 3 \frac{\mu}{r^5} \mathbf{S}(\mathbf{r}^i) \mathbf{J} \mathbf{r}^i.$$

The atmospheric drag can be expressed as [10]

$$\mathbf{f}_{atm}^b = \mathbf{R}_o^b \mathbf{C}_a^o \begin{bmatrix} 0 \\ -\frac{1}{2} \rho v^2 C_d A \\ 0 \end{bmatrix},$$

where ρ is the atmospheric density, v is the spacecraft velocity, C_d is the drag coefficient and \mathbf{C}_a^o as in (2), and $\mathbf{f} \in \mathbb{R}^3$ denotes an translational acceleration vector working on the spacecraft. The J_2 effect is caused by non-homogeneous mass distribution of a planet, and for Earth a simplified model can according to [11] be expressed as

$$\mathbf{f}_{grav}^b = \frac{3}{2} \mu J_2 R_e^2 \mathbf{R}_i^b \begin{bmatrix} 5 \frac{r_x r_z^2}{r^7} - 3 \frac{r_z^3}{r^5} \\ 5 \frac{r_y r_z^2}{r^7} - \frac{r_y}{r^5} \\ 5 \frac{r_z^3}{r^7} - 3 \frac{r_z}{r^5} \end{bmatrix},$$

where $J_2 = 1082.6 \cdot 10^{-6}$ and R_e is the mean equatorial radius of the Earth. The rotational torque caused by perturbing forces can be found from the relation [7]

$$\tau_j^b = \mathbf{S}(\mathbf{r}_c^b) \mathbf{f}_j^b,$$

where \mathbf{r}_c^b is the vector from the spacecraft center of mass to the line of action of the force. Hence the total disturbance torque may be written as

$$\tau_d^b = \tau_{gg}^b + \mathbf{S}(\mathbf{r}_c^b)(\mathbf{f}_{atm}^b + \mathbf{f}_{grav}^b).$$

III. CONTROL OF RIGID BODY

A. Problem Formulation

The control problem is to steer the state $\mathbf{q}(t)$ towards a given reference trajectory $\mathbf{q}_d(t)$ satisfying the kinematic equation

$$\dot{\mathbf{q}}_d = \mathbf{T}(\mathbf{q}_d) \boldsymbol{\omega}_d.$$

The tracking error in quaternion coordinates, $\tilde{\mathbf{q}} = [\tilde{\eta}, \tilde{\boldsymbol{\epsilon}}^\top]^\top$ is given by

$$\tilde{\mathbf{q}} := \mathbf{q} \otimes \bar{\mathbf{q}}_d = \begin{bmatrix} \eta \eta_d + \boldsymbol{\epsilon}^\top \boldsymbol{\epsilon}_d \\ \eta_d \boldsymbol{\epsilon} - \eta \boldsymbol{\epsilon}_d - \mathbf{S}(\boldsymbol{\epsilon}) \boldsymbol{\epsilon}_d \end{bmatrix},$$

and the quaternion velocities may be expressed as (cf. [12])

$$\dot{\tilde{\mathbf{q}}} = \mathbf{T}(\tilde{\mathbf{q}}) (\boldsymbol{\omega} - \boldsymbol{\omega}_d).$$

For the purpose of establishing meaningful stability properties we define the error functions

$$\mathbf{e}_{q\pm} = [1 \mp \tilde{\eta}, \tilde{\boldsymbol{\epsilon}}^\top]^\top, \quad \mathbf{e}_\omega = \boldsymbol{\omega} - \boldsymbol{\omega}_d.$$

Moreover, we have

$$\dot{\mathbf{e}}_{q\pm} = \mathbf{T}_e(\mathbf{e}_{q\pm}) \mathbf{e}_\omega, \quad (7)$$

where

$$\mathbf{T}_e(\mathbf{e}_{q\pm}) = \frac{1}{2} \begin{bmatrix} \pm \tilde{\boldsymbol{\epsilon}}^\top \\ \tilde{\eta} \mathbf{I} + \mathbf{S}(\tilde{\boldsymbol{\epsilon}}) \end{bmatrix}.$$

Remark 3.1: Due to the redundancy implicit to the quaternion representation, $\tilde{\mathbf{q}}$ and $-\tilde{\mathbf{q}}$ represent the same physical attitude but correspond to different equilibria. That is; the two attitude positions differ by a rotation of 2π rad about an arbitrary axis. Consequently, in quaternion coordinates it is not appropriate to speak of global stability properties. This has often been overlooked in the literature.

B. Uniform Asymptotic Stabilization

Assume, for the time-being that the disturbances τ_d^b are known. Consider the PD+ control law

$$\tau_a^b = \mathbf{J} \boldsymbol{\omega}_d - \mathbf{S}(\mathbf{J} \boldsymbol{\omega}) \boldsymbol{\omega}_d - \tau_d - k_p \mathbf{T}_e^\top \mathbf{e}_q - k_d \mathbf{e}_\omega. \quad (8)$$

The following proposition establishes uniform asymptotic stability of the closed-loop system under a modified PD+ controller.

Proposition 3.1: Let \mathbf{e}_q be defined either by $\mathbf{e}_q = \mathbf{e}_{q+}$ or $\mathbf{e}_q = \mathbf{e}_{q-}$ and respectively, let $\tilde{\eta}(t_0) \geq 0$ or $\tilde{\eta}(t_0) < 0$, and assume that $\text{sgn}(\tilde{\eta}(t_0)) = \text{sgn}(\tilde{\eta}(t))$ for all $t > t_0$,

and assume that the desired attitude $\mathbf{q}_d(t)$, desired angular velocity $\boldsymbol{\omega}_d(t)$ and the desired angular acceleration $\dot{\boldsymbol{\omega}}_d(t)$ are all bounded functions. The dual equilibrium points $(\mathbf{e}_{q\pm}, \mathbf{e}_\omega) = (\mathbf{0}, \mathbf{0})$ of the system (4) and (5), in closed-loop with the control law

$$\begin{aligned} \tau_a^b &= \mathbf{J} \dot{\boldsymbol{\omega}}_d - \mathbf{S}(\mathbf{J} \boldsymbol{\omega}) \boldsymbol{\omega}_d - \tau_d^b \\ &\quad - k_p e^{k_1 \mathbf{e}_q^\top \mathbf{e}_q} \mathbf{T}_e^\top \mathbf{e}_q - k_d e^{k_2 \mathbf{e}_\omega^\top \mathbf{e}_\omega} \mathbf{e}_\omega, \end{aligned} \quad (9)$$

where $k_p > 0$, $k_d > 0$, $k_1 > 0$ and $k_2 > 0$ are feedback gains, are uniformly asymptotically stable (UAS).

Proof: Without loss of generality, we show stability of the positive equilibrium point i.e., let $\mathbf{e}_q = \mathbf{e}_{q+}$ and $\mathbf{T}_e = \mathbf{T}_e(\mathbf{e}_{q+})$.

The closed-loop dynamics that results from substituting (9) in (5) is

$$\begin{aligned} \dot{\mathbf{e}}_\omega &= \mathbf{J}^{-1} \left(\mathbf{S}(\mathbf{J} \boldsymbol{\omega}) \mathbf{e}_\omega \right. \\ &\quad \left. - k_p e^{k_1 \mathbf{e}_q^\top \mathbf{e}_q} \mathbf{T}_e^\top \mathbf{e}_q - k_d e^{k_2 \mathbf{e}_\omega^\top \mathbf{e}_\omega} \mathbf{e}_\omega \right). \end{aligned} \quad (10)$$

Consider the radially unbounded and positive definite Lyapunov function candidate

$$V(\mathbf{x}) = \frac{1}{2} \left[\frac{k_p}{k_1} \left(e^{k_1 \mathbf{e}_q^\top \mathbf{e}_q} - 1 \right) + \mathbf{e}_\omega^\top \mathbf{J} \mathbf{e}_\omega \right], \quad (11)$$

with lower and upper bounds

$$\begin{aligned} \underline{\kappa}(\|\mathbf{x}\|) &= \frac{1}{2} \min \left\{ \frac{k_p}{k_1}, j_m \right\} \|\mathbf{x}\|^2 \\ \bar{\kappa}(\|\mathbf{x}\|) &= \frac{1}{2} \max \left\{ \frac{k_p}{k_1}, j_M \right\} \left(e^{k_1 \|\mathbf{x}\|^2} - 1 \right) \end{aligned}$$

where $\mathbf{x} = [\mathbf{e}_q^\top, \mathbf{e}_\omega^\top]^\top$, $j_m \leq \|\mathbf{J}\| \leq j_M$. The total time derivative of V along the closed-loop trajectories generated by (7) and (10) yields

$$\begin{aligned} \dot{V}(\mathbf{x}) &= k_p e^{k_1 \mathbf{e}_q^\top \mathbf{e}_q} \mathbf{e}_q^\top \mathbf{T}_e \mathbf{e}_\omega + \mathbf{e}_\omega^\top \mathbf{S}(\mathbf{J} \boldsymbol{\omega}) \mathbf{e}_\omega \\ &\quad - \mathbf{e}_\omega^\top k_p e^{k_1 \mathbf{e}_q^\top \mathbf{e}_q} \mathbf{T}_e^\top \mathbf{e}_q - \mathbf{e}_\omega^\top k_d e^{k_2 \mathbf{e}_\omega^\top \mathbf{e}_\omega} \mathbf{e}_\omega \\ &= - \mathbf{e}_\omega^\top k_d e^{k_2 \mathbf{e}_\omega^\top \mathbf{e}_\omega} \mathbf{e}_\omega \\ &\leq - \mathbf{e}_\omega^\top k_d \mathbf{e}_\omega \leq 0. \end{aligned}$$

where we have used that $k_2 > 0$ and $\mathbf{S}(\mathbf{J} \boldsymbol{\omega})$ is skew-symmetric. We conclude that the equilibrium point $(\mathbf{e}_q, \mathbf{e}_\omega) = (\mathbf{0}, \mathbf{0})$ is uniformly stable and the solutions are uniformly bounded.

For uniform asymptotic stability we invoke Matrosov's theorem as stated in [2]. To that end, we introduce the auxiliary function

$$W(\mathbf{x}) = \mathbf{e}_q^\top \mathbf{T}_e \mathbf{J} \mathbf{e}_\omega$$

which is continuous and uniformly bounded on compacts of the state. The total time derivative of W along closed-loop

trajectories yields

$$\dot{W}(\mathbf{x}) = \dot{\mathbf{e}}_q^\top \mathbf{T}_e \mathbf{J} \mathbf{e}_\omega + \mathbf{e}_q^\top \dot{\mathbf{T}}_e \mathbf{J} \mathbf{e}_\omega + \mathbf{e}_q^\top \mathbf{T}_e \mathbf{J} \dot{\mathbf{e}}_\omega \quad (12)$$

$$\begin{aligned} &= \mathbf{e}_\omega^\top \mathbf{T}_e^\top \mathbf{T}_e \mathbf{J} \mathbf{e}_\omega + \mathbf{e}_q^\top \dot{\mathbf{T}}_e \mathbf{J} \mathbf{e}_\omega \\ &\quad - \mathbf{e}_q^\top \mathbf{T}_e \left[\left(-\mathbf{S}(\mathbf{J}\omega) + k_d e^{k_2 \mathbf{e}_\omega^\top \mathbf{e}_\omega} \mathbf{I} \right) \mathbf{e}_\omega \right. \\ &\quad \left. + k_p e^{k_1 \mathbf{e}_q^\top \mathbf{e}_q} \mathbf{T}_e^\top \mathbf{e}_q \right]. \end{aligned} \quad (13)$$

We now verify that \dot{W} is non-zero definite on the set $E = \{\dot{V} = 0\} = \{\mathbf{e}_\omega = \mathbf{0}\}$. To that end observe that

$$\mathbf{e}_\omega = \mathbf{0} \Rightarrow \dot{W}(\mathbf{x}) = -\mathbf{e}_q^\top \mathbf{T}_e k_p e^{k_1 \mathbf{e}_q^\top \mathbf{e}_q} \mathbf{T}_e^\top \mathbf{e}_q. \quad (14)$$

We claim that

$$\dot{W}(\mathbf{x}) \leq -\mathbf{e}_q^\top \frac{k_p}{8} \mathbf{e}_q. \quad (15)$$

To see this we first notice that

$$\mathbf{e}_q^\top \mathbf{T}_e \mathbf{T}_e^\top \mathbf{e}_q = \frac{1}{4} \tilde{\epsilon}^\top \tilde{\epsilon} \quad (16)$$

Also, in view of (7) we have

$$\frac{1}{8} \left((1 - \tilde{\eta})^2 + \tilde{\epsilon}^\top \tilde{\epsilon} \right) = \frac{1}{8} \mathbf{e}_q^\top \mathbf{e}_q.$$

Now, assume that

$$\frac{1}{4} \tilde{\epsilon}^\top \tilde{\epsilon} < \frac{1}{8} \left((1 - \tilde{\eta})^2 + \tilde{\epsilon}^\top \tilde{\epsilon} \right) \quad (17)$$

which is equivalent to

$$(1 - \tilde{\eta})^2 > \tilde{\epsilon}^\top \tilde{\epsilon}. \quad (18)$$

In view of the quaternion constraint $\tilde{\epsilon}^\top \tilde{\epsilon} = 1 - \tilde{\eta}^2$ inequality (18) holds if and only if $2\tilde{\eta}(1 - \tilde{\eta}) > 0$. In its turn, the latter holds only if $\tilde{\eta} < 0$ or $\tilde{\eta} > 1$. However, this does not hold by assumption *i.e.*, $\tilde{\eta} \in [0, 1]$. We conclude that (17) does not hold. Therefore, from (16)–(18) we obtain that

$$\mathbf{e}_q^\top \mathbf{T}_e \mathbf{T}_e^\top \mathbf{e}_q \geq \frac{1}{8} \mathbf{e}_q^\top \mathbf{e}_q$$

which together with (14) and $k_1 \geq 0$ implies (15). That is, \dot{W} is non-zero definite on E . Uniform asymptotic stability follows invoking Matrosov's theorem.

The proof for the negative equilibrium point \mathbf{e}_{q-} , $\mathbf{T}_e(\mathbf{e}_{q-})$ follows along the same lines. We conclude that the dual equilibrium points $(\mathbf{e}_{q\pm}, \mathbf{e}_\omega) = (\mathbf{0}, \mathbf{0})$ are uniformly asymptotically stable. \square

C. Uniform Practical Asymptotic Stability

In the previous section, uniform asymptotic stability clearly follows under the assumption that τ_a^b is known and accounted for in the control law. In this section we relax this assumption and assume that τ_a^b is unknown, but bounded. More precisely, we assume that there exists $\beta_d > 0$ such that $\|\tau_a^b\| \leq \beta_d$.

Proposition 3.2: *Let \mathbf{e}_q be defined either by $\mathbf{e}_q = \mathbf{e}_{q+}$ or $\mathbf{e}_q = \mathbf{e}_{q-}$ and respectively, let $\tilde{\eta}(t_0) \geq 0$ or $\tilde{\eta}(t_0) < 0$. Assume that $\text{sgn}(\tilde{\eta}(t_0)) = \text{sgn}(\tilde{\eta}(t))$ for all $t > t_0$. Assume further that the desired attitude $\mathbf{q}_d(t)$, desired angular*

velocity $\omega_d(t)$ and the desired angular acceleration $\dot{\omega}_d(t)$ are all bounded functions. Then, the dual equilibrium points $(\mathbf{e}_{q\pm}, \mathbf{e}_\omega) = (\mathbf{0}, \mathbf{0})$ of the system (4) and (5), in closed loop with the control law

$$\begin{aligned} \tau_a^b &= \mathbf{J} \dot{\omega}_d - \mathbf{S}(\mathbf{J}\omega) \omega_d \\ &\quad - k_p e^{k_1 \mathbf{e}_q^\top \mathbf{e}_q} \mathbf{T}_e^\top \mathbf{e}_q - k_d e^{k_2 \mathbf{e}_\omega^\top \mathbf{e}_\omega} \mathbf{e}_\omega, \end{aligned} \quad (19)$$

where $k_p > 0$, $k_d > 0$, $k_1 > 0$ and $k_2 > 0$ are feedback gains, are uniformly practically asymptotically stable (UPAS).

Proof: We start by considering the positive equilibrium point such that $\mathbf{e}_q = \mathbf{e}_{q+}$ and $\mathbf{T}_e = \mathbf{T}_e(\mathbf{e}_{q+})$. By inserting the control law (19) into (5) we obtain the closed-loop dynamics

$$\begin{aligned} \dot{\mathbf{e}}_\omega &= \mathbf{J}^{-1} \left(\mathbf{S}(\mathbf{J}\omega) \mathbf{e}_\omega - k_p e^{k_1 \mathbf{e}_q^\top \mathbf{e}_q} \mathbf{T}_e^\top \mathbf{e}_q \right. \\ &\quad \left. - k_d e^{k_2 \mathbf{e}_\omega^\top \mathbf{e}_\omega} \mathbf{e}_\omega + \tau_a^b \right). \end{aligned} \quad (20)$$

The total time derivative of V defined in (11) along the closed-loop trajectories generated by (7) and (20) yields

$$\dot{V} \leq -\mathbf{e}_\omega^\top k_d \mathbf{e}_\omega + \beta_d \|\mathbf{e}_\omega\|. \quad (21)$$

Let $\delta := \beta_d/k_d$. From the expression above, we have $\dot{V} < 0$ if $\|\mathbf{e}_\omega\| > \delta$. Since V is positive definite and proper we obtain that $\|\mathbf{e}_\omega(t)\|$ is bounded that is, for any $r > 0$ there exists $\Delta(r) > 0$ such that $\sup_{t \geq t_0} \|\mathbf{e}_\omega(t)\| \leq \Delta$ for all initial conditions $\|\mathbf{x}(t_0)\| < r$, $t_0 \geq 0$.

For any Δ , let $\lambda(\Delta) > 0$ be a constant to be determined. Consider the Lyapunov function candidate

$$\mathcal{V}(\mathbf{x}) = V(\mathbf{x}) + \lambda W(\mathbf{x})$$

which is positive definite and proper for $\lambda \leq 1$. Its total time derivative along the closed-loop trajectories yields

$$\begin{aligned} \dot{\mathcal{V}}(\mathbf{x}) &= -\mathbf{e}_\omega^\top k_d e^{k_2 \mathbf{e}_\omega^\top \mathbf{e}_\omega} \mathbf{e}_\omega + \beta_d \|\mathbf{e}_\omega\| + \lambda \mathbf{e}_\omega^\top \mathbf{T}_e^\top \mathbf{T}_e \mathbf{J} \mathbf{e}_\omega \\ &\quad + \lambda \mathbf{e}_q^\top \dot{\mathbf{T}}_e \mathbf{J} \mathbf{e}_\omega + \lambda \mathbf{e}_q^\top \mathbf{T}_e \left(\mathbf{S}(\mathbf{J}\omega) - k_d e^{k_2 \mathbf{e}_\omega^\top \mathbf{e}_\omega} \mathbf{I} \right) \mathbf{e}_\omega \\ &\quad - \lambda \mathbf{e}_q^\top \mathbf{T}_e k_p e^{k_1 \mathbf{e}_q^\top \mathbf{e}_q} \mathbf{T}_e^\top \mathbf{e}_q + \lambda \beta_d \|\mathbf{e}_q\|. \end{aligned}$$

By inserting $\dot{\mathbf{T}}_e \mathbf{e}_q = \mathbf{G}(\tilde{\mathbf{q}}) \mathbf{e}_\omega$, where $\mathbf{G}(\tilde{\mathbf{q}}) = 1/2[\tilde{\eta} \mathbf{I} + \mathbf{S}(\tilde{\epsilon})] - \mathbf{I}/4$, and notice that $\|\mathbf{T}_e^\top \mathbf{T}_e\| = \mathbf{I}/4$ and $\|\mathbf{e}_q \mathbf{T}_e^\top\| \leq \|\mathbf{e}_q\|$, we obtain

$$\begin{aligned} \dot{\mathcal{V}}(\mathbf{x}) &\leq -\mathbf{e}_\omega^\top k_d e^{k_2 \mathbf{e}_\omega^\top \mathbf{e}_\omega} \mathbf{e}_\omega + \frac{\lambda}{2} \mathbf{e}_\omega^\top [\tilde{\eta} \mathbf{I} + \mathbf{S}(\tilde{\epsilon})] \mathbf{J} \mathbf{e}_\omega \\ &\quad + \lambda \mathbf{e}_q^\top \mathbf{T}_e \left(\mathbf{S}(\mathbf{J}\omega) - k_d e^{k_2 \mathbf{e}_\omega^\top \mathbf{e}_\omega} \mathbf{I} \right) \mathbf{e}_\omega \\ &\quad - \lambda \mathbf{e}_q^\top \mathbf{T}_e k_p e^{k_1 \mathbf{e}_q^\top \mathbf{e}_q} \mathbf{T}_e^\top \mathbf{e}_q + 2\beta_d \|\mathbf{x}\| \\ &= -\mathbf{x}^\top \mathbf{P} \mathbf{x} + 2\beta_d \|\mathbf{x}\|, \end{aligned}$$

where we defined $\mathbf{P} = [\mathbf{p}_{ij}]$, $i, j = 1, 2$ with

$$\begin{aligned} \mathbf{p}_{11} &= k_d e^{k_2 \mathbf{e}_\omega^\top \mathbf{e}_\omega} \mathbf{I} - \frac{\lambda}{2} [\tilde{\eta} \mathbf{I} + \mathbf{S}(\tilde{\epsilon})] \mathbf{J} \\ \mathbf{p}_{12} &= \mathbf{p}_{21}^\top = \frac{\lambda}{2} \mathbf{T}_e^\top \left(-\mathbf{S}(\mathbf{J}\omega) + k_d e^{k_2 \mathbf{e}_\omega^\top \mathbf{e}_\omega} \mathbf{I} \right) \\ \mathbf{p}_{22} &= \lambda \mathbf{T}_e k_p e^{k_1 \mathbf{e}_q^\top \mathbf{e}_q} \mathbf{T}_e^\top. \end{aligned}$$

Notice that for any $\|\mathbf{e}_\omega\| \leq \Delta$ and $\|\boldsymbol{\omega}_d\| \leq \beta_{\omega_d}$ which hold under the arguments made so far, the angular velocities $\boldsymbol{\omega} = \mathbf{e}_\omega + \boldsymbol{\omega}_d$ satisfy the bound $\|\boldsymbol{\omega}\| \leq \zeta(\Delta, \beta_{\omega_d})$ for some number $\zeta > 0$. Therefore, $\|\mathbf{S}(\mathbf{J}\boldsymbol{\omega})\| \leq \zeta(\Delta, \beta_{\omega_d}, j_M)$ for some number $\tilde{\zeta} > 0$.

Next, we use $2|ab| \leq a^2 + b^2$ for any $a, b \in \mathbb{R}$ to obtain

$$\mathbf{x}^\top \mathbf{P} \mathbf{x} \geq (p_{11,m} - p_{12,M}) \|\mathbf{e}_q\|^2 + (p_{22,m} - p_{12,M}) \|\mathbf{e}_\omega\|^2$$

where $p_{ij,m}$ and $p_{ij,M}$ denote lower and upper bounds on the induced norms of the sub-blocks \mathbf{p}_{ij} of \mathbf{P} respectively. Hence,

$$p_{11,m} \geq 2p_{12,M}, \quad p_{22,m} \geq 2p_{12,M}, \quad (22)$$

resulting in

$$\mathbf{x}^\top \mathbf{P} \mathbf{x} \geq \frac{1}{2} (p_{11,m} \|\mathbf{e}_q\|^2 + p_{22,m} \|\mathbf{e}_\omega\|^2).$$

To fulfill (22) we need to choose

$$\lambda \leq \frac{2k_d}{\tilde{\zeta}(\Delta, \beta_{\omega_d}, j_M) + k_d e^{k_2 \Delta^2} + j_M}$$

$$k_p \geq 2 \left[\tilde{\zeta}(\Delta, \beta_{\omega_d}, j_M) + k_d e^{k_2 \Delta^2} \right],$$

Thus,

$$\dot{\mathbf{V}} \leq -p_m \|\mathbf{x}\|^2 + 2\beta_d \|\mathbf{x}\|,$$

where $p_m > 0$ is a uniform lower bound on the smallest eigenvalue of $\mathbf{P}(\cdot)$. The derivative $\dot{\mathbf{V}} < 0$ for all states such that $\|\mathbf{x}\| > \delta' := 2\beta_d/p_m$. Note that p_m depends on the controller gains monotonically hence the closed-loop trajectories system converge from any ball of initial conditions in the state space to a ball in close vicinity of the origin, of radius δ' . Moreover, the latter may be reduced at will by increasing the control gains. We conclude that the equilibrium point $(\mathbf{e}_q, \mathbf{e}_\omega) \rightarrow (\mathbf{0}, \mathbf{0})$ is uniformly practically asymptotically stable.

The proof for the negative equilibrium point \mathbf{e}_{q-} , $\mathbf{T}_e(\mathbf{e}_{q-})$ follows along similar lines hence, the dual equilibrium points $(\mathbf{e}_{q\pm}, \mathbf{e}_\omega) = (\mathbf{0}, \mathbf{0})$ are uniformly practically asymptotically stable. \square

IV. SIMULATION RESULTS

We present now some simulation results for a spacecraft on an elliptic LEO. The simulations were performed in Simulink using a variable sample-time Runge-Kutta ODE45 solver with relative and absolute tolerance of 10^{-9} . The moments of inertia were chosen as $\mathbf{J} = \text{diag}\{4.35, 4.33, 3.664\}$ kgm², and the spacecraft orbit was chosen with perigee at 600 km, apogee at 750 km, inclination at 71°, and the argument of perigee and the right ascension of the ascending node at 0°.

For sake of comparison, we performed simulations using the PD+ controller

$$\boldsymbol{\tau}_a^b = \mathbf{J}\dot{\boldsymbol{\omega}}_d - \mathbf{S}(\mathbf{J}\boldsymbol{\omega})\boldsymbol{\omega}_d - k_p \mathbf{T}_e^\top \mathbf{e}_q - k_d \mathbf{e}_\omega. \quad (23)$$

TABLE I

VALUES OF PERFORMANCE FUNCTIONALS FOR ATTITUDE MANEUVER

	J_q	J_ω	J_p
PD+	4.202	0.767	2.409
PD+ w/exponentially gains	4.015	0.765	2.719

TABLE II

VALUES OF PERFORMANCE FUNCTIONALS FOR ATTITUDE MANEUVER OVER ONE ORBITAL PERIOD (5896 s)

	J_q	J_ω	J_p
PD+	4.489	0.850	6.476
PD+ w/exponentially gains	4.171	0.797	3.961

as well as the modified PD+ controller. To evaluate and compare the performance of the controllers we use the functionals

$$J_q = \int_{t_0}^{t_f} \tilde{\boldsymbol{\epsilon}}^\top \tilde{\boldsymbol{\epsilon}} dt, \quad J_\omega = \int_{t_0}^{t_f} \mathbf{e}_\omega^\top \mathbf{e}_\omega dt, \quad J_p = \int_{t_0}^{t_f} \boldsymbol{\tau}_a^\top \boldsymbol{\tau}_a dt,$$

where t_0 and t_f defines the start and end of the simulation window, respectively. The functional J_q and J_ω describes the integral functional error of the attitude and angular velocity error, while J_p describes the integral of the applied control torque.

We introduce measurement noise as $\sigma \mathbb{B}^n = \{x \in \mathbb{R}^n : \|x\| \leq \sigma\}$ and add a suitable amount to the error functions according to $\tilde{\mathbf{e}}_q = (\mathbf{e}_q + 0.05\mathbb{B}^4)/\|\mathbf{e}_q + 0.05\mathbb{B}^4\|$ and $\tilde{\mathbf{e}}_\omega = \mathbf{e}_\omega + 0.01\mathbb{B}^3$ which represent a poor spacecraft navigational system. Disturbances are added according to Section II-D with $\mathbf{r}_c^b = [0.1, 0, 0]^\top$. For our simulations we have chosen the initial conditions as $\mathbf{q} = [-0.3772, -0.4329, 0.6645, 0.4783]^\top$ and $\boldsymbol{\omega} = [0.1, -0.3, 0.2]^\top$, $t_0 = 0$ s, $t_f = 30$ s. The control laws were tuned to achieve similar performance for sake of comparison thus using parameters $k_p = k_d = 2$ for (23), and $k_p = 1, k_d = 1.6$ and $k_1 = k_2 = 1$ for (19).

The simulation results are summarized in Table I and depicted in Figure 1. The performance functionals show that both controllers have similar performance though the ordinary controller has slightly higher attitude and angular velocity error while the power consumption is slightly lower.

The simulation results for one orbital period (5896 s) is presented in Table II and as can be seen the performance functionals are less affected for (19) compared to (23). This is because as $\mathbf{e}_q \approx \mathbf{0}$ and $\mathbf{e}_\omega \approx \mathbf{0}$, the controller gains for (19) are $k_p e^{k_1 \mathbf{e}_q^\top \mathbf{e}_q} \approx k_p$ and $k_d e^{k_2 \mathbf{e}_\omega^\top \mathbf{e}_\omega} \approx k_d$ and since the gains k_p and k_d are smaller for (19) compared to (23) for a similar maneuver, the noise has less effect on the performance functionals.

In table III we present simulation results from a wide number of simulations for a general rigid-body without disturbances and noise with controller gains $k_p = 2, k_d = 1$ for both (8) and (9), and using random initial values for the quaternion vector, while the initial angular velocity was found randomly with standard deviation in equal steps from

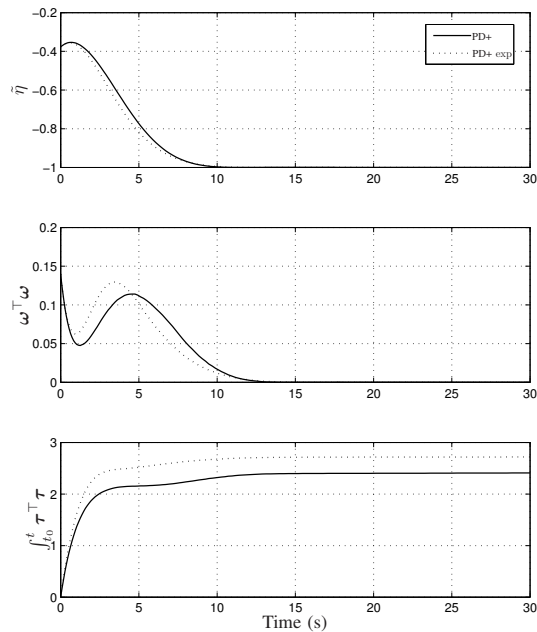


Fig. 1. Attitude and angular velocity error, and power consumption using PD+ and PD+ with exponentially gain controllers during spacecraft attitude maneuver.

TABLE III

AVERAGE VALUE OF PERFORMANCE FUNCTIONALS FOR RIGID-BODY OVER 10,000 SIMULATIONS

	J_q	J_ω	J_p
PD+	2.060	0.947	2.140
PD+ w/exponentially gains	1.382	0.916	4.174

0.01 to 0.5 rad/s during 10,000 consecutive runs. This is done to show that the exponential gains makes the system work faster than constant gains, for the price of increased power consumption.

V. CONCLUSION

We improved the existing PD+ control law by introducing exponentially proportional and derivative gains for control of a rigid body. It was showed that the equilibria of the closed-loop system with known disturbances are uniformly asymptotically stable and uniformly practically asymptotically stable under the effect of disturbances. Simulation results show that, in terms of integrated error and power consumption the proposed controller is much less affected by sensor noise. Simulations also show that the proposed controller in general works faster than the ordinary PD+ controller with an increase in power consumption.

REFERENCES

[1] R. Ortega, A. Loria, P. J. Nicklasson, and H. Sira-Ramírez, *Passivity-based Control of Euler-Lagrange Systems: Mechanical, Electrical and*

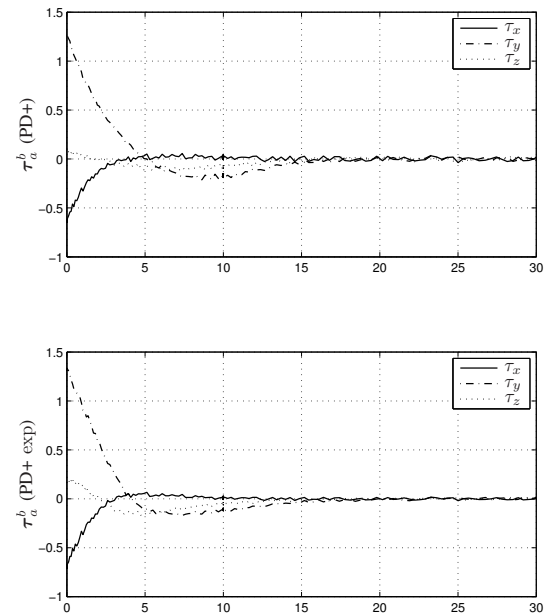


Fig. 2. Control torque using PD+ and PD+ with exponentially gains controllers during spacecraft attitude maneuver.

[2] B. Paden and R. Panja, "Globally asymptotically stable 'PD+' controller for robot manipulators," *International Journal of Control*, vol. 47, no. 6, pp. 1697–1712, 1988.

[3] J. J.-E. Slotine and W. Li, "On the adaptive control of robot manipulators," *International Journal of Robotics Research*, vol. 6, pp. 49–59, 1987.

[4] J. T.-Y. Wen and K. Kreutz-Delgado, "The attitude control problem," *IEEE Transactions on Automatic Control*, vol. 36, no. 10, pp. 1148–1162, 1991.

[5] R. Kristiansen, *Dynamic Synchronization of Spacecraft - Modeling and Coordinated Control of Leader-Follower Spacecraft Formations*. PhD thesis, Department of Engineering Cybernetics, Norwegian University of Science and Technology, Trondheim, Norway, 2008.

[6] H. Schaub and J. L. Junkins, *Analytical Mechanics of Space Systems*. AIAA Education Series, Reston, VA: American Institute of Aeronautics and Astronautics, 2003. ISBN 1-56347-563-4.

[7] O. Egeland and J. T. Gravdahl, *Modeling and Simulation for Automatic Control*. Trondheim, Norway: Marine Cybernetics, 2002. ISBN 82-92356-01-0.

[8] M. J. Sidi, *Spacecraft Dynamics and Control*. New York: Cambridge University Press, 1997. ISBN 0-521-78780-7.

[9] Ø. Hegrenæs, J. T. Gravdahl, and P. Tøndel, "Spacecraft attitude control using explicit model predictive control," *Automatica*, vol. 41, pp. 2107–2114, 2005.

[10] J. R. Wertz, ed., *Spacecraft Attitude Determination and Control*. London: Kluwer Academic Publishers, 1978. ISBN 90-277-0959-9.

[11] O. Montenbruck and E. Gill, *Satellite Orbits. Models, methods, applications*. Berlin, Germany: Springer-Verlag, 2001. First edition, corrected second printing, ISBN 3-540-67280-X.

[12] O.-E. Fjellstad, *Control of Unmanned Underwater Vehicles in Six Degrees of Freedom*. PhD thesis, Department of Engineering Cybernetics, Norwegian University of Science and Technology, Trondheim, Norway, 1994.